

Military Technical College,
Kobry El-Kobbah,
Cairo, Egypt



9th International Conference
On Aerospace Sciences &
Aviation Technology

PERFORMANCE ANALYSIS OF MACRO-, MICRO- AND PICO-CELLULAR DS/CDMA MOBILE RADIO SYSTEMS

Al-Shennawy* H. A., Mourad** H. M., Al-Bassiouni*** A. M.
and Al-Hussaini**** E. K.

ABSTRACT

A generalized model is presented for comparative analysis of the reverse link (i.e. from the mobile station (MS) to the cell site (CS)) of macro-, micro- and pico-cellular mobile radio systems employing conventional correlator receiver (CCR), and microscopic diversity of CCRs. This paper analyses the systems error probabilities considering both sectorization and voice activity monitoring. The multiple access interference (MAI) and noise are assumed zero mean Gaussian random variable. The interrelationships among the number of interfering cells, sectorization degree, voice activity factor, sectorization imperfection and the number of users are described. This paper confirms that when using CCR, pico-cells yield the best performance and micro-cells yield better performance than macro-cells. The amount of MAI has a substantial effect on the performance. It is shown also that MAI can be reduced by sectorization and voice activity monitoring. Using microscopic diversity of CCRs also improves the systems performance.

KEY WORDS

DS/CDMA, cellular systems, sectorization, voice activity monitoring and microscopic diversity.

*Egyptian Armed forces

** Dr. Electronics and Communications Dept., Faculty of Engineering, Cairo University

*** Lucent Technologies, Cairo.

****Prof. Dr. Electronics and Communications Dept., Faculty of Engineering, Cairo University

1. INTRODUCTION

Direct sequence code division multiple access (DS/CDMA) has drawn the attention of researchers for its application in cellular and personal communication system (PCS). In previous studies [1]-[4], single cell systems were analyzed and only interfering users in the home cell was taken into account. In the literature, some papers analyzed the performance of macro-cellular mobile radio systems for e.g. [5]-[7], while others analyzed the performance of micro-cellular mobile radio systems for e.g. [8]-[10]. In [8] a comparative analysis of macro-, micro-, and pico-cellular for a slotted CDMA systems was presented in terms of the throughput and delay and only the first tier of interfering cells was taken into account. In this paper a comparative analysis of macro-, micro-, and pico-cellular DS/CDMA systems in terms of the average probability of error using a generalized mathematical model. Multiple cell systems employing CCR and microscopic diversity of CCRs and using binary phase shift keying (BPSK) are analyzed. The effect of interfering MSs from both home cell and surrounding cells are taken into account. Multipath fading, path loss, additive white Gaussian noise (AWGN), MAI and sectorization imperfection are considered. Voice activity monitoring and sectorization are suggested to improve the performance.

This paper is organized as follows: In section (2), the system model is introduced. In section (3), the performance of DS/CDMA macro, micro and pico-cellular mobile radio systems employing CCR, microscopic diversity of CCRs is analyzed. The effects of interfering cells, sectorization degree, sectorization imperfection, on/voice activity monitoring and diversity order on the performance are also investigated. Numerical results are presented in section (4). Conclusions are given in section (5).

2. SYSTEM MODEL

In cellular hierarchy, we have N cells, cell#1 is the home cell, the other $N_1=N-1$ are the interfering cells. $N_1=0$ corresponds to single cell system. $N_1=6, 18$ and 36 correspond to multiple cell system with one, two and three tiers of interfering cells. According to the size of the cells, we get macro-, micro- and pico-cellular systems. Macro-cellular systems are used in low user density areas for instance in rural areas and suburban areas. Micro-cellular systems are used in high-density areas such as urban areas, city centers, highways, shopping malls, and airport areas. Pico-cellular are suitable for indoor communications (e.g. offices, modern factories, research laboratories, hospitals, university campuses, etc.). Macro-cells are of large size (2-20 km diameter) with the antenna radiating large power (0.6-10 W) from the top of tall buildings. Micro-cells are relatively much smaller in size (0.4-2 km diameter) with their antennas at street lamp elevations operating at relatively low power (less than 20 mW). Pico-cells are the smallest size (20-400 m diameter), with antenna placed on top of a bookshelf and radiating power of a few mW.

2.1 Channel model

The channel's impulse response is given by:

$$h(t) = \sum_{m=1}^M \alpha_{mk} e^{-j\theta_{mk}} \delta(t - \tau_{mk}) \quad (1)$$

where M is the number of paths, α_{mk} , τ_{mk} and θ_{mk} are the path gain, the path delay and the path phase for the k^{th} user at the m^{th} path respectively. We assume that: the path phases are independent and identically distributed random variables uniformly distributed over $[0, 2\pi]$. The path time delays are independent and identically

distributed random variables uniformly distributed over $[0, T_b]$ where T_b is the bit duration. All the path time delays and phases are independent of one another and independent of data and path amplitudes. The propagation path loss of the received signal amplitude is uniformly distributed in $(0, 1)$. The path gains are independent and identically distributed random variables. In micro- and pico-cellular, the probability density function (pdf) of the desired signal amplitude envelope is given by:

$$p_r(r) = \frac{r}{\sigma_m^2} \exp\left(-\frac{r^2 + s^2}{2\sigma_m^2}\right) I_0\left(\frac{rs}{\sigma_m^2}\right) \quad 0 \leq r \leq \infty \quad (2)$$

where 'r' is the signal amplitude, σ_m^2 is the average fading power, s is the peak value of the directly received signal, $I_0(\cdot)$ is the modified Bessel function of the first kind and zero order. The Rician distribution is characterized by the Rice factor R, which is defined as the ratio of the average direct power to the average fading power and can be written as:

$$R = \frac{s^2}{2\sigma_m^2} \quad (3)$$

Typical values for 'R' in micro-cells are 7dB and 12 dB. In pico-cells 'R' equals 6.8 and 11 dB depending on the type and construction material of the buildings [1]. Assuming that 's'=1, the signal power envelope probability density function (pdf) is modeled by:

$$f_p(p) = 2R \exp(-R[2p+1]) I_0(2R\sqrt{2p}) \quad p \geq 0 \quad (4)$$

Macro-cellular system is modeled by Rayleigh fading channel [7] and [8] due to the relatively large size of the cell. Rician fading degenerates into Rayleigh fading when no line of sight exists i.e. 's'= 0 then 'R'= 0. The received signal amplitude envelope pdf is given by:

$$f_r(r) = \frac{r}{2\sigma_m^2} \exp\left(-\frac{r^2}{2\sigma_m^2}\right) \quad r \geq 0 \quad (5)$$

The signal power envelope pdf is given by:

$$f_p(p) = \frac{1}{\sigma_m^2} \exp\left(-\frac{p}{\sigma_m^2}\right) \quad p \geq 0 \quad (6)$$

It is assumed also that the number of resolvable paths is fixed and upper bounded by [8]:

$$M = \left\lceil \frac{T_m}{T_c} \right\rceil + 1 \quad (7)$$

where $\lceil x \rceil$ is the largest integer that is less than or equal to x, T_c is the chip

duration and T_m is the root mean square (rms) delay spread. In macro-cells, T_m is in the order of 8 microseconds. In micro-cells, T_m is in the order of 2 microseconds. In pico-cells, T_m ranges from 50 to 250 nanoseconds [8].

In micro-cellular environment, At short distance, low antenna height, with MS antenna height=1.5 m and CS antenna height =5-20 m at frequency f=870.15MHz, signal attenuation are measured for a MS moving along busy city streets in a direction radial to CS. Measurements [11]-[13] approved that the path loss is characterized by dual path-loss model defined by two slopes: close to the CS, the slope is 'a₁', where the propagation may be guided by buildings. Near the cell boundary, the slope is 'a₁+b₁' due to the combined effects of ground/buildings reflections and interception of first Fresnel ellipsoid. a₁=2 and b₁ =2-8. The received signal power p_r at the CS is given by:

$$p_r = p_t c \left[\frac{1}{d^{a_1} (1 + \frac{d}{g})^{b_1}} \right] \quad (8)$$

where p_t is the average transmitted power from the MS, 'd' is the distance between the CS and the MS, 'g' is the turning point which is determined by the CS and the MS antennas heights and the operating frequency. It equals 100-200 meters. 'c' is a constant that determines the offset moving the signal up and down and describes the average level of the signal. It equals 37-94.7 depending on antenna heights [8]. In both macro- and pico- cellular systems, the path loss is characterized by single path-loss model [1], [7] and [10]:

$$p_r = p_t c \left[\frac{1}{d^{a_1}} \right] \quad (9)$$

A lot of measurements have been done to obtain information about the value of the path loss law exponent 'a₁' in practical indoor environments. The path loss exponent a₁<2 if the CS and the MSs are positioned in the same hallway in an office building due to the waveguiding effects in the hallway. a₁=3, if the MSs are in rooms which are located off the same hallway containing the CS. a₁= 4 up to 6, if the MSs are in rooms off a hallway perpendicular to the CS' hallway. a₁=6, in buildings with metalized partions. Factory buildings have few internal partions. Aisles are arranged orderly, intersecting fashion and are flanked by metal machinery or inventory and storage racks. Ceilings and walls are made of ribbed steel and metal ceiling trusswork is used. In factories, a₁=1.79 up to 2 in case of line of sight (LOS) path for both light and heavy clutter of the surroundings (machinery and storage racks) [1] and [14]. The value of a₁ also depends on the morphology of the building. In our analysis a₁=2 is assumed. In macro-cellular systems path loss exponent 'a₁' ranges from 3 to 5 (typically 4) [7] and [14].

2.2 'On' and 'voice' activity monitoring

During a two-person conversation, each person is not active all the time but remains silent for a certain percentage of the time. Previous studies show that each speaker is active only 35% to 40% of the time and listens the rest of the time. Recent studies show that this activity is higher in mobile environment than in wire line and can have values between 50 and 60 %. When no voice activity monitoring is used "a" =1. When voice activity monitoring is used "a" =0.7 or 0.5 or 0.3. Typically the voice activity factor "a" is 3/8. DS/CDMA capacity is interference limited thus any reduction in interference converts directly and linearly into an increase in capacity. If voice activity is monitored and transmission is suppressed or squelched when no voice is present, MAI is reduced and the system capacity increases. The number of users per

each cell is K . When using 'on' activity monitoring, the probability that K_1 out of K users are "on" can be described by a binomial distribution: [15], [16]

$$p(K, K_1) = \binom{K}{K_1} b^{K_1} (1-b)^{K-K_1} \quad (10a)$$

where 'b' is 'on' activity factor. When using 'voice' activity monitoring, the probability that K_2 out of K_1 "on" users is active can be described by a binomial distribution:

$$p(K_1, K_2) = \binom{K_1}{K_2} a^{K_2} (1-a)^{K_1-K_2} \quad (10b)$$

where 'a' is voice activity factor, which is defined as the ratio of the time the MS is active to the total period of time. Since K is sufficiently large, we approximate the average number of "on" users who are talking as:

$$MS_{avg} = abK. \quad (10c)$$

2.3 Sectorization

Sectorization [15] refers to dividing the cell into 3 or 6 sectors and using 3 or 6 directional antennas at the CS each having 120 or 60 degree effective beamwidth instead of an omnidirectional antenna. Let D be the sectorization degree ($D=3$ or 6). The MAI experienced at the CS of an ideal sectorized cell is $1/D$ of an omniscell.

2.4 Sectorization imperfection

When using ideal directional antennas, there is a sharp separation between the sectors. The antenna gain is assumed equal throughout the sector. Outside the sector, a gain of zero is assumed. The gain of realistic directional antenna of a sector is less uniform. It radiates power outside its sector and it receives some interference from users in other sectors, due to overlap and side lobe anomalies. The real antenna pattern must be described by a parabolic function but analogous to the method for describing noise by the noise equivalent bandwidth, we assume that the gain of the antenna is constant over the home sector plus a part of the adjacent sectors. This part is determined by the overlap angle. The overlap angle is measured from the sector boundaries. The overlap angle depends on the antenna type. We assume also that the antenna gain is zero at angles larger than the overlap angle. We describe the real antenna pattern by a uniform function. The effect of imperfect sectorization is modeled by the overlap angle ν . The interference correction factor due to imperfect sectorization F_s is defined as the ratio of the total interference power received in a sectorized cell system and the total interference power received in an omniscell cell system [15].

$$F_s = (1/D + 2\nu/360) \quad (11)$$

In case of omniscell system (i.e. no sectorization) $D=1$ and $\nu=0$. In case of perfect sectorization $D=3$ or 6 and $\nu=0$. In case of imperfect sectorization $D=3$ or 6 and ν varies up to 35°

3. PERFORMANCE ANALYSIS

The MAI and noise are considered zero mean Gaussian random variables. The signal to interference plus noise ratio (SINR) can be derived as (see appendix A):

$$SINR = \frac{P}{\frac{N_0}{2E_b} + (\sigma_m^2 + \frac{s^2}{2}) \frac{2F_s}{3L} [(1 + \frac{N_1}{c_1})abMK - 1]} \quad (12)$$

where E_b/N_0 is the energy per bit-to-noise power spectral density ratio, L is the processing gain $L = T_b/T_c = 1/R_b T_c$ where R_b is the data rate and 's' is the value of the directly received signal. In macro-cellular 's'=0 and 'c₁'=5, in micro-cellular 's'=1 and 'c₁'=10 and in pico-cellular 's'=1 and 'c₁'=3.

3.1 The conventional correlator receiver (CCR)

The block diagram of the CCR is shown in Fig. (1-a). Where $r_{MU}(t)$ is the received signal, $\hat{b}(t)$ is the decision variable and the subscript MU refers to multi users. The average probability of error of BPSK is given by:

$$P(e) = \int_0^\infty Q(\sqrt{SINR}) f_p(p) dp \quad (13)$$

After some mathematical manipulations, the average probability of error in macro-cellular is given by [7]:

$$P(e) = \frac{1}{2} \left[1 - \frac{1}{\left[1 + \frac{N_0}{2E_b \sigma_m^2} + \frac{2F_s}{3L} \left[(1 + \frac{N_1}{5})abMK - 1 \right] \right]^{\frac{1}{2}}} \right] \quad (14)$$

While in micro-cellular and pico-cellular, it is given by:

$$P(e) = \int_0^\infty Q\left(\sqrt{\frac{P}{\frac{N_0}{2E_b} + \frac{1}{2R}(1+R) \frac{2F_s}{3L} \left[(1 + \frac{N_1}{c_1})abMK - 1 \right]}} \right) f_p(p) dp \quad (15)$$

3.2 Microscopic diversity of CCRs

Microscopic diversity is a very efficient technique to mitigate the effects of multipath fading. The term micro is used because decorrelation between the received signals occurs if the separation between the antennas is about one-half wavelength (typically less than one foot for frequency above 500 MHz). Microscopic diversity reception is equivalent to space diversity utilizing different antennas at the same CS. The antennas should be separated by distances long enough to obtain independent fast fading components. Using selection combining, the branch with highest signal is selected to set up communication with the MS. The block diagram of the microscopic

diversity with CCRs is shown in Fig. (1b). The pdf of the strongest output in micro and pico-cellular can be derived as [14] and [17]:

$$f_{\alpha \max}(p) = d_1 \left(1 - Q_1(2\sqrt{pR}, 2\sqrt{R})\right)^{d_1-1} 2R \exp(-R[2p+1]) I_0(2R\sqrt{2p}) \quad (16)$$

where d_1 is the diversity order and $Q_1(a,b)$ is the Marcum Q-function which is defined by:

$$Q_1(a,b) = \int_0^\infty x \exp\left(-\frac{x^2+a^2}{2}\right) I_0(ax) dx$$

while in macro-cellular, the pdf of the strongest output can be derived as:

$$f_{\alpha \max}(p) = d_1 \left(1 - \exp\left(-\frac{p}{\sigma_m^2}\right)\right)^{d_1-1} \frac{1}{\sigma_m^2} \exp\left(-\frac{p}{\sigma_m^2}\right) \quad (17)$$

Finally the average probability of error is given by:

$$P(e) = \int_0^\infty Q(\sqrt{SINR}) f_{\alpha \max}(p) dp \quad (18)$$

4. NUMERICAL RESULTS

All figures confirm that pico-cells outperform the two other systems and that the performance degrades with the increase of the number of users. Fig. 2 shows the effect of MAI on the system performance. The performance of single cell systems ($N_1=0$) and multiple cell systems ($N_1=36$) is considered. It is shown that the average probability of error increases as the number of interfering cells N_1 taken into consideration increases. Fig. 3 illustrates the influence of on/voice activity monitoring on the average probability of error. The performance of the three cellular systems without voice activity monitoring ($a=1$) and with voice activity monitoring ($a=3/8$) is considered. It is shown that as the voice activity factor increases, the average probability of error increases. Fig. 4 demonstrates the influence of sectorization on the average probability of error. The performance of the three cellular systems without sectorization ($D=1$) and with sectorization ($D=3$) is considered. It is shown that the average probability of error decreases and the number of users simultaneously supported by the system K increases with increasing D . Fig. 5 depicts the effect of imperfect sectorization. It is shown that when sectorization is perfect, the average probability of error decreases with the decrease of 'D'. It is also shown that as the overlap angle increases, the system performance degrades. Fig. 6 depicts the performance of the three cellular systems without microscopic diversity ($d_1=1$) and with microscopic diversity ($d_1=3$) using CCRs. It is shown that microscopic diversity improves the performance of the three cellular systems. Furthermore, the performance saturates to the same average probability of error for sufficiently large number of users since the effect of MAI dominates that of fading and noise.

5. CONCLUSIONS

A generalized mathematical model for analyzing macro-, micro-, and pico-cellular systems employing CCR is introduced. It is observed that due to the smallest rms delay spread, pico-cells yield the best performance. As expected, the multiple cell systems have inferior bit error probabilities compared with single cell systems due to

the interference introduced by the surrounding cells. The performance deteriorates with the increase of number of users and the overlap angle. However, microscopic diversity of CCRs, sectorization and voice activity monitoring substantially improve the system performance.

REFERENCES

- [1] R. Prasad, H. S. Misser and A. Kegel "Performance evaluation of direct-sequence spread spectrum multipath-access for indoor wireless communication in Rician fading channel" IEEE Trans. Commun. Vol. 43, pp. 581-592, February/March/April 1995.
- [2] M. B. Pursely "Performance evaluation for phase-coded spread-spectrum multiple access communication- Part 1: system analysis " IEEE trans. Commun. Vol. Com-25, No. 8, pp. 795-799, August 1977.
- [3] F. Simpson and J. M. Holtzman "Direct sequence CDMA power control, interleaving and coding " IEEE J. Select Areas Commun. Vol. 11, No.7, pp.1085 - 1095, September 1993.
- [4] R. Cameron and B. Woerner "Performance analysis of CDMA with imperfect power control" IEEE trans. Commun. Vol.44, No.7, pp.777-781, July 1996.
- [5] R. Prasad and A. Kegel "Improved assessment of interference limits in cellular radio performance" IEEE trans. Veh. Technol. Vol. 40, No.2, pp. 412-419, May 1991.
- [6] O. K. Tongues and M. M. Wang "Cellular CDMA network impaired by Rayleigh fading system performance with power control" IEEE Trans. Veh. Technol. Vol. 43, No.3, pp.515-526, August 1994.
- [7] J. Mar and H. Yi Chen "Performance analysis of cellular CDMA networks over frequency selective fading channel" IEEE Trans. Veh. Technol. Vol. 47, No.4, pp. 1234-1244, November 1998.
- [8] C. A. F. J. Wjffels, H. S. Misser and R. Prasad "A micro-cellular CDMD over slow and fast Rician fading radio channels with forward error correcting coding and diversity " IEEE trans. Veh. Technol. Vol. 42, No.4, pp.570-580, November 1993.
- [9] Yu Dong Yao and A. U. H. Sheikh" Investigation into cochannel interference in microcellular mobile radio systems" IEEE Trans. veh. Technol. vol. 41, No 2, PP. 114-123, May 1992.
- [10] R. Prasad and A. Kegel "Effects of Rician faded and log-normal shadowed signals on spectrum efficiency in microcellular radio" IEEE trans. Veh. Technol. Vol. 42, No. 3, PP. 274-281, August 1993.
- [11] P. Harely "Short distance attenuation measurements at 900 MHz and 1.8 GHz using low antenna heights for microcells " IEEE J. select. Area commun. Vol.7, pp.5-10, Jan. 1989.
- [12] H. H. Xia, H. L. Bertoni, L. R. Maciel, A. L. Stewart, and R. Rowe "Radio propagation characteristics for line-of-sight microcellular and personal communications" IEEE Trans. Antennas Propagat. Vol. 41, No. 10, PP.1439 - 1447, Oct. 1993.
- [13] R. J. C. Bultitude and G. K. Bedal "Propagation characteristics on microcellular urban mobile radio channels at 910 MHz" IEEE select area commun. Vol. 7, No. 1, pp. 31-39, Jan. 1989
- [14] R. Prasad "CDMA for wireless personal communications" Artech House, Boston, London 1996.
- [15] M. G. Jansen and R. Prasad "Capacity, throughput and delay analysis of a cellular DS/CDMA system with imperfect power control and imperfect sectorization" IEEE trans. Veh. Technol. Vol. 44, No.1, PP. 67-74, Feb. 1995.

- [16] R. L. Pickholyz, L. B. Milstein and D.L. Schilling, "Spread spectrum for mobile communications", IEEE Trans. Veh. Technol. Vol. 40, No.2, PP 313-321, May 1991.
 [17] T. Proakis, "Digital communication", New York, McGraw Hill, 3rd Ed., 1995.

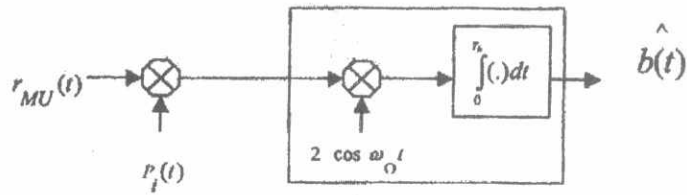


Fig. 1a. The block diagram of the conventional correlator receiver (CCR)

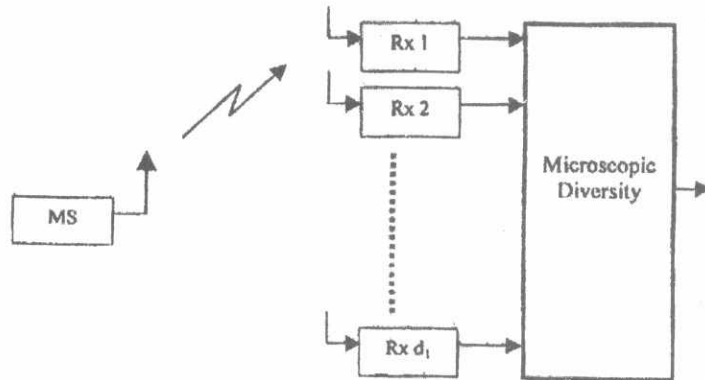


Fig. 1b Block diagram of microscopic diversity reception

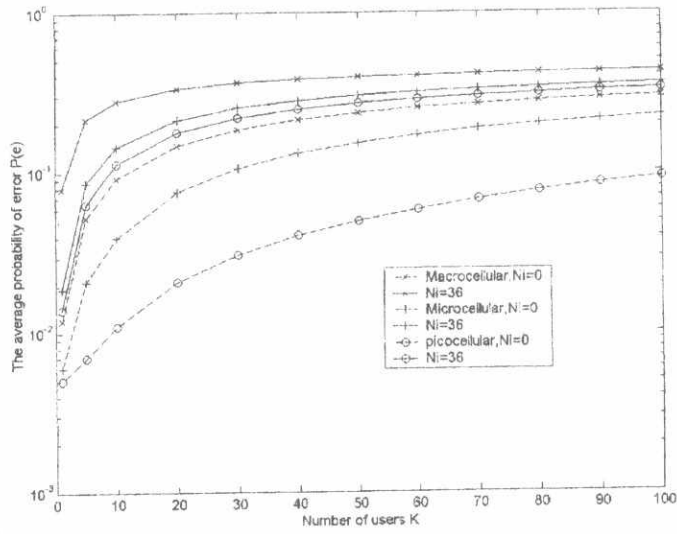


Fig. 2 Performance of the three cellular systems for single cell systems and three tiers cells systems ($L=127, R_b=32\text{ kbit/s}, D=3, b=0.8, a=3/8, E_b/N_o=20\text{ dB}, v=0$) (a) **macro-cells**, $T_m=8\text{ us}, R=0, M=32$ (b) **micro-cells**, $T_m=2\text{ us}, R=7\text{ dB}, M=8$ (c) **pico-cells**, $T_m=185\text{ ns}, R=6.8\text{ dB}, M=2$).

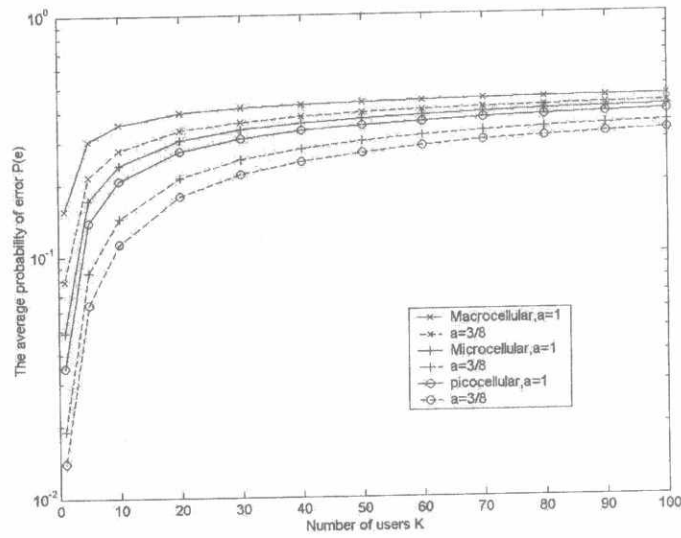


Fig. 3 Performance of the three cellular systems with and without voice activity monitoring ($L=127, R_b=32\text{ kbit/s}, b=0.8, N_f=36, D=3, E_b/N_0=20\text{ dB}, v=0$), (a) **macro-cells**, $T_m=8\text{ us}, R=0, M=32$ (b) **micro-cells**, $T_m=2\text{ us}, R=7\text{ dB}, M=8$ (c) **pico-cells**, $T_m=185\text{ ns}, R=6.8\text{ dB}, M=2$).

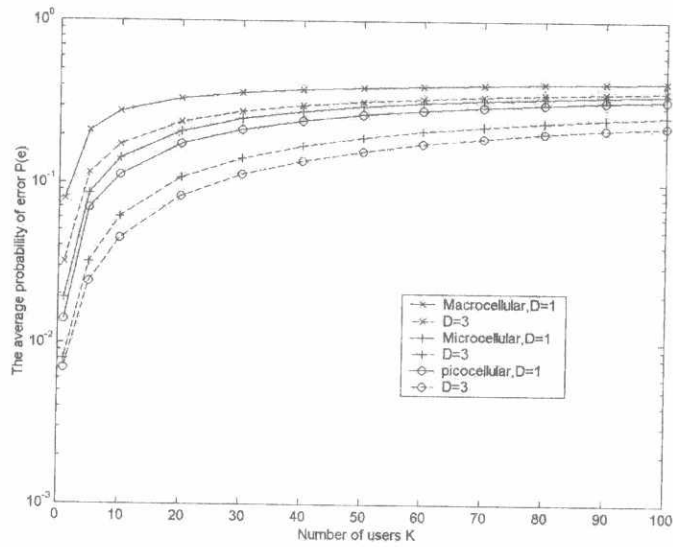


Fig. 4 Performance of the three cellular systems with and without sectorization ($L=127$, $R_b=32$ kbit/s, $b=0.8$, $a=3/8$, $N_1=36$, $E_b/N_0=20$ dB, $v=0$, (a) **macro-cells**, $T_m=8$ us, $R=0$, $M=32$ (b) **micro-cells**, $T_m=2$ us, $R=7$ dB, $M=8$ (c) **pico-cells**, $T_m=185$ ns, $R=6.8$ dB, $M=2$).

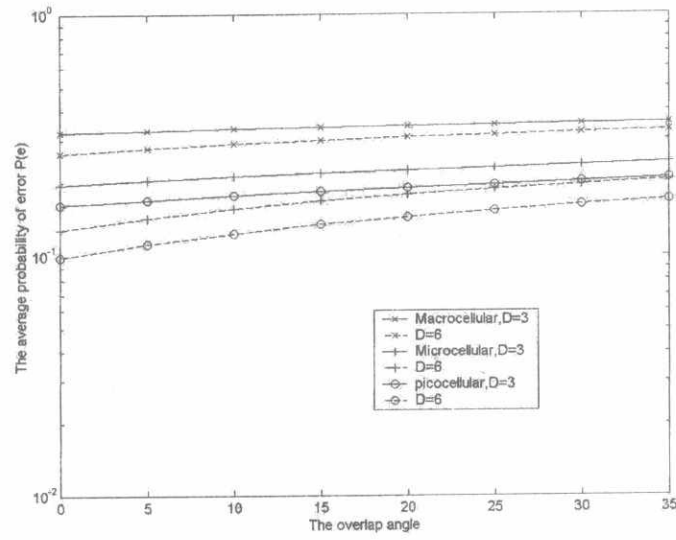


Fig. 5 shows the effect of imperfect sectorization upon the three cellular systems. ($L=127$, $R_b=32$ kbit/s, $K=50$, $b=0.8$, $a=3/8$, $N_1=36$, $E_b/N_0=20$ dB, $\nu=0$, (a) **macro-cells**, $T_m=8$ us, $R=0$, $M=32$ (b) **micro-cells**, $T_m=2$ us, $R=7$ dB, $M=8$ (c) **pico-cells**, $T_m=185$ ns, $R=6.8$ dB, $M=2$.)

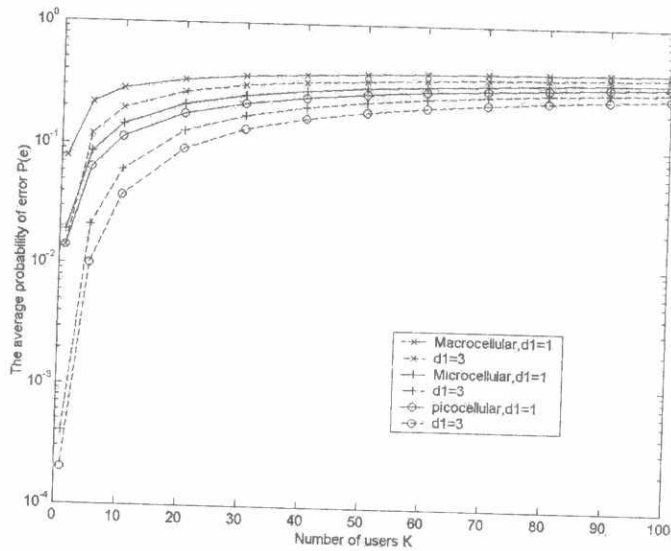


Fig. 6 Performance of the three cellular systems with and without microscopic diversity. ($L=127, R_b=32\text{ kbit/s}, D=3, b=0.8, a=3/8, N_f=36, E_b/N_o=20\text{ dB}, v=0$, (a) **macro-cells**, $T_m=8\text{ }\mu\text{s}, R=0, M=32$ (b) **micro-cells**, $T_m=2\text{ }\mu\text{s}, R=7\text{ dB}, M=8$ (c) **pico-cells**, $T_m=185\text{ ns}, R=6.8\text{ dB}, M=2$.)

Appendix A

Derivation of Eqn. (12)

The received signal at the CS of cell #1 can be expressed as:

$$r(t) = \sum_{m=1}^M \sum_{k_1=1}^K A \alpha_{m,k_1} P_{k_1}(t - \tau_{m,k_1}) b_{k_1}(t - \tau_{m,k_1}) \cos(\omega_0 t + \phi_{m,k_1}) + \sum_{n=2}^N \sum_{m_n=1}^M \sum_{k_n=1}^K A \alpha_{m_n,k_n} \beta_{k_n}^2 b_{k_n}(t - \tau_{m_n,k_n}) P_{k_n}(t - \tau_{m_n,k_n}) \cos(\omega_0 t + \phi_{m_n,k_n}) + n(t) \quad (A.1)$$

where

α_{m,k_1} and α_{m_n,k_n} are the fading factors for the k^{th} user's signal at the m^{th} path of cell #1 and cell #n respectively.

p_{k_1} and p_{k_n} are the codes of the k^{th} user of cell #1 and cell #n.

b_{k_1} and b_{k_n} are the k^{th} user's data signal of cell #1 and cell #n.

A is the amplitude of the transmitted signal.

τ_{m,k_1} , τ_{m_n,k_n} , θ_{m,k_1} and θ_{m_n,k_n} represent the time delays and carrier phases of the k^{th} user's signal of cell #1 and cell #n.

$$\phi_{m,k_1} = \theta_{m,k_1} - \omega_0 \tau_{m,k_1}$$

$$\phi_{m_n,k_n} = \theta_{m_n,k_n} - \omega_0 \tau_{m_n,k_n}$$

$\beta_{k_n}^2$ describes how the received signal power falls off with distance.

In case of micro - cellular, using eqn.(8), we get

$$\beta_{k_n} = \left(\frac{d_{n,k_n}^{-\alpha_1/2} (1 + \frac{d_{n,k_n}}{g})^{-\beta_1/2}}{d_{1,k_n}^{-\alpha_1/2} (1 + \frac{d_{1,k_n}}{g})^{-\beta_1/2}} \right)$$

In case of macro - cellular and in case of pico - cellular, using eqn.(9), we get

$$\beta_{k_n} = \left(\frac{d_{n,k_n}}{d_{1,k_n}} \right)^{\alpha_1/2}$$

where

d_{1,k_n} and d_{n,k_n} are the distances from the CS of cell #1 and cell #n respectively to the k^{th} user of cell #n.

β_{k_n} is uniformly distributed in [0, 1]

$n(t)$ is additive white Gaussian noise (AWGN) having two sided power spectral density $N_0 / 2$.

The test statistic can be written as:

$$Z(T_b) = D(T_b) + I_S(T_b) + I_{ICU}(T_b) + I_{OCU}(T_b) + N(T_b) \quad (A.2)$$

where

$D(T_b)$ the k th user desired signal term

$$D(T_b) = \pm AT_b \alpha_{ii} \quad (A.3)$$

$I_S(T_b)$ the i^{th} user self interference term (interpath interference(IPI) or multipath interference (MPI)).

$$I_S(T_b) = \sum_{\substack{m_i=1 \\ m_i \neq i}}^M A \alpha_{m_i k_i} \int_0^{T_b} b_{k_i}(t - \tau_{m_i k_i}) P_{K_i}(t - \tau_{m_i k_i}) P_i(t) \cos \phi_{m_i k_i} dt \quad (A.4)$$

$I_{ICU}(T_b)$ the i^{th} user internal cell users interference term.

$$I_{ICU}(T_b) = \sum_{\substack{m_i=1 \\ k_i \neq i}}^M \sum_{k_i=1}^K A \alpha_{m_i i} \int_0^{T_b} P_{K_i}(t - \tau_{m_i k_i}) b_{k_i}(t - \tau_{m_i k_i}) P_i(t) \cos \phi_{m_i k_i} dt \quad (A.5)$$

$I_{OCU}(T_b)$ the i^{th} user outer cell users interference term.

$$I_{OCU}(T_b) = \sum_{n=2}^N \sum_{m_n=1}^M \sum_{k_n=1}^K \alpha_{m_n k_n} \beta_{k_n}^2 \int_0^{T_b} b_{k_n}(t - \tau_{m_n k_n}) P_{K_n}(t - \tau_{m_n k_n}) P_i(t) \cos \phi_{m_n k_n} dt \quad (A.6)$$

$N(T_b)$ the output noise signal term .

$$N(T_b) = \int_0^{T_b} n(t) P_i(t) 2 \cos \omega_0 t dt \quad (A.7)$$

The MAI is the sum of the following four terms

$$I(T_b) = I_S(T_b) + I_{ICU}(T_b) + I_{OCU}(T_b) + N(T_b) \quad (A.8)$$

When the number of users is sufficiently large, the MAI can be approximated as Gaussian random variable with zero mean.

Let

$$I_{k_i}(T_b) = \int_0^{T_b} P_{K_i}(t - \tau_{m_i k_i}) b_{k_i}(t - \tau_{m_i k_i}) P_i(t) dt$$

$$I_{k_n}(T_b) = \int_0^{T_b} b_{k_n}(t - \tau_{m_n k_n}) P_{K_n}(t - \tau_{m_n k_n}) P_i(t) dt$$

$$\text{Then } E\{I_{k_i}^2(T_b)\} = E\{I_{k_n}^2(T_b)\} = \frac{2T_b^2}{3L}$$

$$E\{\alpha_{m_i k_i}^2\} = E\{\alpha_{m_n k_n}^2\} = (2\sigma_m^2 + s^2)$$

$$E\{\cos^2 \phi_{m,k_1}\} = E\{\cos^2 \phi_{m,k_n}\} = \frac{1}{2}, \quad E\{\beta_{nk}^2\} = \frac{1}{5} \text{ in case of macro-cellular,}$$

$$E\{\beta_{nk}^2\} = \frac{1}{10} \text{ in case of micro-cellular, } E\{\beta_{nk}^2\} = \frac{1}{3} \text{ in case of pico-cellular}$$

$$\text{var}\{I_S(T_b)\} = E\{I_S^2(T_b)\} = A^2(M-1)E\{\alpha_{m,k_1}^2\}E\{\cos^2 \phi_{m,k_1}\}E\{I_{k_1}^2(T_b)\}$$

$$= A^2(M-1)(2\sigma_m^2 + s^2)\left(\frac{1}{2}\right)\left(\frac{2T_b^2}{3L}\right) \quad (\text{A.9})$$

$$\text{var}\{I_{ICU}(T_b)\} = E\{I_{ICU}^2(T_b)\} = A^2M(K-1)E\{\alpha_{m,k_1}^2\}E\{\cos^2 \phi_{m,k_1}\}E\{I_{k_1}^2(T_b)\}$$

$$= A^2M(K-1)(2\sigma_m^2 + s^2)\left(\frac{1}{2}\right)\left(\frac{2T_b^2}{3L}\right) \quad (\text{A.10})$$

$$\text{var}\{I_{OCU}(T_b)\} = E\{I_{OCU}^2(T_b)\} = A^2MK(N-1)E\{\alpha_{m,k_n}^2\}E\{\cos^2 \phi_{m,k_n}\}E\{I_{k_n}^2(T_b)\}E\{\beta_{nk}^2\}$$

$$= A^2MK(N-1)(2\sigma_m^2 + s^2)\left(\frac{1}{2}\right)\left(\frac{2T_b^2}{3L}\right)\left(\frac{1}{c_1}\right) \quad (\text{A.11})$$

$$\text{var}\{N(T_b)\} = E\{N^2(T_b)\} = N_0T_b \quad (\text{A.12})$$

$$E\{I^2(T_b)\} = A^2\left(\sigma_m^2 + \frac{s^2}{2}\right)\frac{2T_b^2}{3L}\left[M-1+MK-M+\frac{N_1}{c_1}MK\right] + N_0T_b$$

$$= A^2\left(\sigma_m^2 + \frac{s^2}{2}\right)\frac{2T_b^2}{3L}\left[\left(1+\frac{N_1}{c_1}\right)MK-1\right] + N_0T_b \quad (\text{A.13})$$

$$SINR = \frac{\text{signal power}}{\text{interference power} + \text{noise power}}$$

$$SINR = \frac{A^2T_b^2\alpha_{ii}^2}{A^2\left(\sigma_m^2 + \frac{s^2}{2}\right)\frac{2T_b^2}{3L}\left[\left(1+\frac{N_1}{c_1}\right)MK-1\right] + N_0T_b}$$

$$= \frac{\alpha_{ii}^2}{\frac{2}{3L}\left(\sigma_m^2 + \frac{s^2}{2}\right)\left[\left(1+\frac{N_1}{c_1}\right)MK-1\right] + \frac{N_0T_b}{A^2T_b^2}} \quad (\text{A.14})$$

$$\text{but } E_b = \frac{A^2T_b}{2} \Rightarrow 2E_b = A^2T_b \quad \text{and let } p = \alpha_{ii}^2$$

$$SINR = \frac{p}{\frac{2}{3L}\left(\sigma_m^2 + \frac{s^2}{2}\right)\left[\left(1+\frac{N_1}{c_1}\right)MK-1\right] + \frac{N_0}{2E_b}} \quad (\text{A.15})$$

Using eqn. (10c) - to include on and voice activity - and (11) - to include imperfect setorization - into (A.15), we get :

$$SINR = \frac{p}{\frac{2F_s}{3L}\left(\sigma_m^2 + \frac{s^2}{2}\right)\left[\left(1+\frac{N_1}{c_1}\right)abMK-1\right] + \frac{N_0}{2E_b}} \quad (\text{A.16})$$